

Electronic Supporting Information (ESI)

Real-time measurement of the intracellular pH of yeast cells during glucose metabolism using ratiometric fluorescent nanosensors

Mohamed M Elsutohy, †^a Veeren M Chauhan, †^a Robert Markus, ^b Mohammed Aref Kyyaly, ^{c,d} Saul JB Tendler^{a,e} and Jonathan W Aylott*^a

^aSchool of Pharmacy, Boots Science Building, University of Nottingham, Nottingham, NG7 2RD, UK

^bSchool of Life Sciences, University of Nottingham, Nottingham, NG7 2RD, UK

^cBioenergy and Brewing Science, School of Biosciences, Sutton Bonington Campus, University of Nottingham, Sutton, Leicestershire, LE12 5RD, UK,

^dCurrent Address: Clinical and Experimental Sciences, Faculty of Medicine, Southampton General Hospital, University of Southampton, Southampton, SO16 6YD, UK

^eCurrent Address: Vice-Chancellor's Department, University of York, Heslington, York, YO10 5DD, UK

*Address correspondence to: jon.aylott@nottingham.ac.uk; Fax: +44 (0) 115 9515102

†Authors contributed equally to this work.

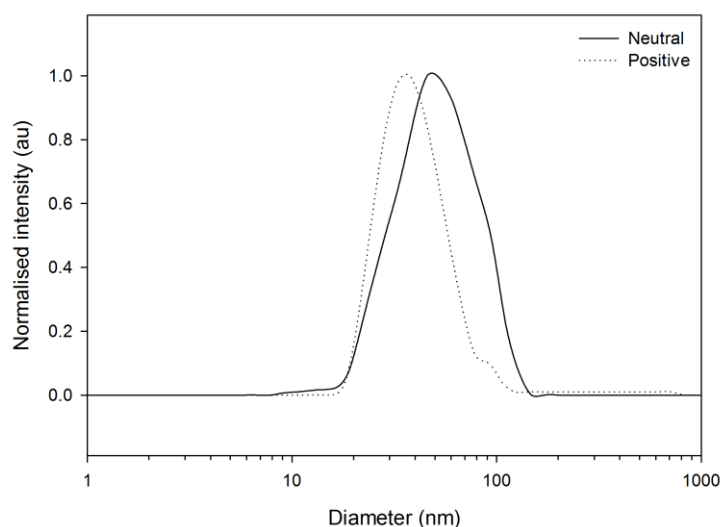


Figure S1: The hydrodynamic diameters for (*solid line*) unmodified/neutral and (*dashed line*) ACTA modified, positively-charged pH-sensitive polyacrylamide nanosensors. ¹ Positive and neutral nanosensors hydrodynamic diameters were centred at 37 nm and 45 nm, respectively.

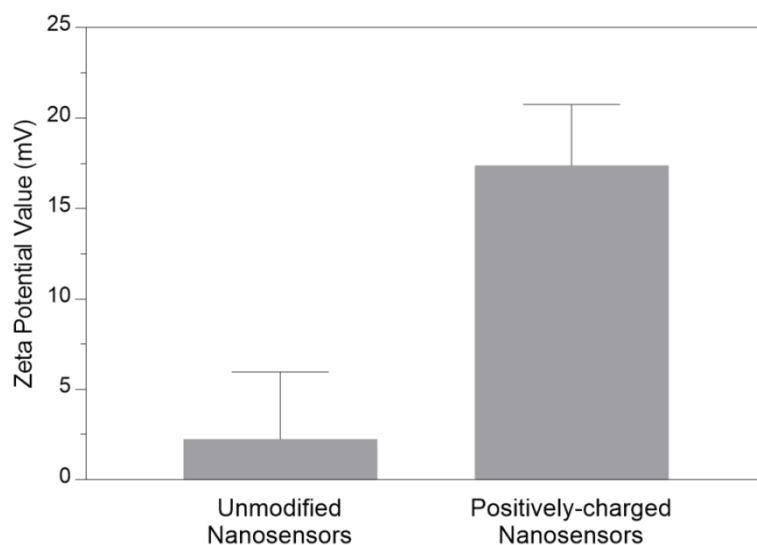


Figure S2: The zeta potential values of unmodified polyacrylamide nanosensors and positively-charged polyacrylamide nanosensors, detected by a Malvern™ DLS instrument. Error bar represent standard deviation measured for different batches of nanoparticles, where n=3.

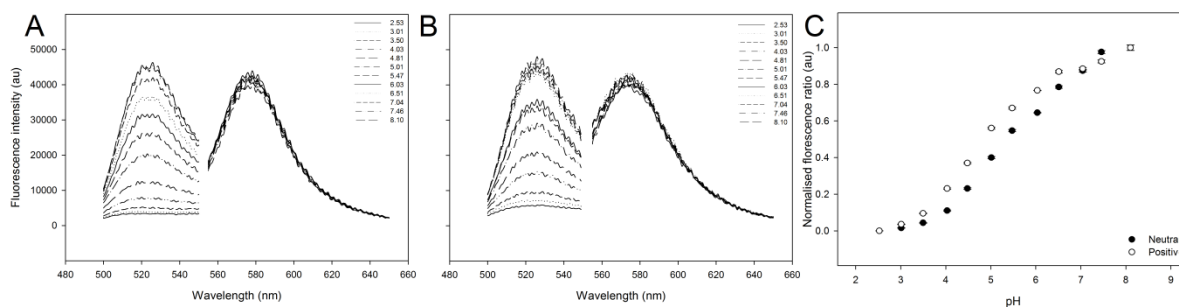


Figure S3. Fluorescence emission curve for (A) neutral and (B) positively-charged, ACTA functionalised, pH sensitive nanosensor, suspended in buffer solutions ranging from pH 2.52 to 8.10. (C) Comparison of normalised calibration curves for neutral and positive particles. Positive nanosensors exhibit a pH calibration curve that is shifted to higher pH values such that the pKa, calculated through derivation of a four parameter sigmoidal pH calibration curve, when compared to the neutral particles is 5.42 and 4.72 respectively. Error bars represent standard deviation (within data points), where n=3 calibration repeats.

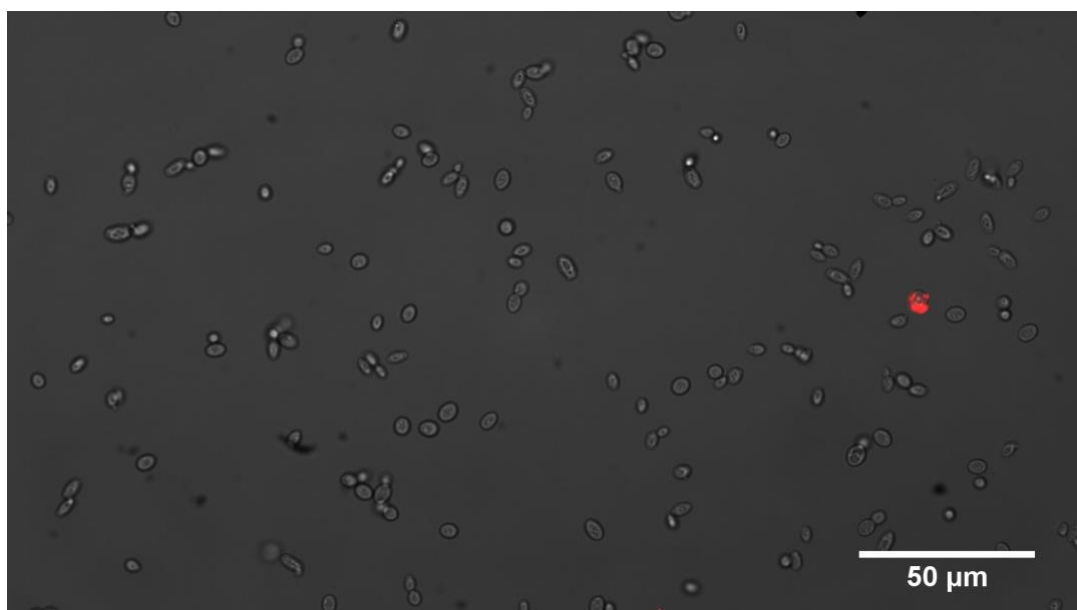


Figure S4: The fluorescent image of yeast cells incubated with unmodified polyacrylamide nanosensors (surface charge of 2.26 ± 3.7 mV). The image was taken in the brightfield mode and red channel of the fluorescence microscope and shows that none of yeast cells were internalised with unmodified nanosensors.

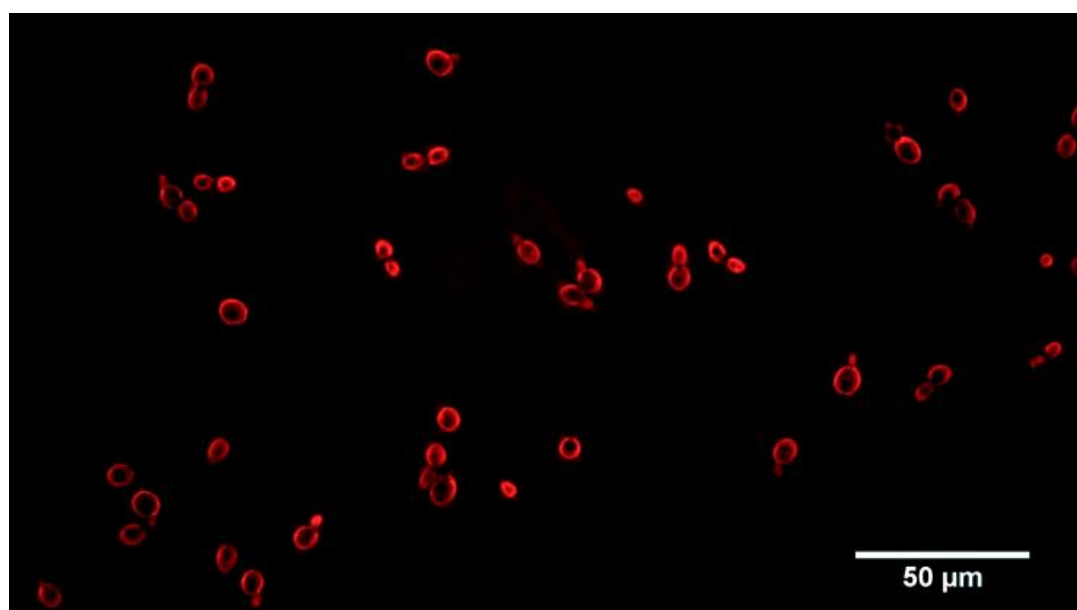


Figure S5: The fluorescent image of yeast cells incubated with unmodified polyacrylamide nanosensors using hyperosmotic sodium chloride method². The image was taken in the brightfield mode and red channel of the fluorescence microscope which shows that all yeast cells were incorporated with nanosensors however, cells were morphologically abnormal.

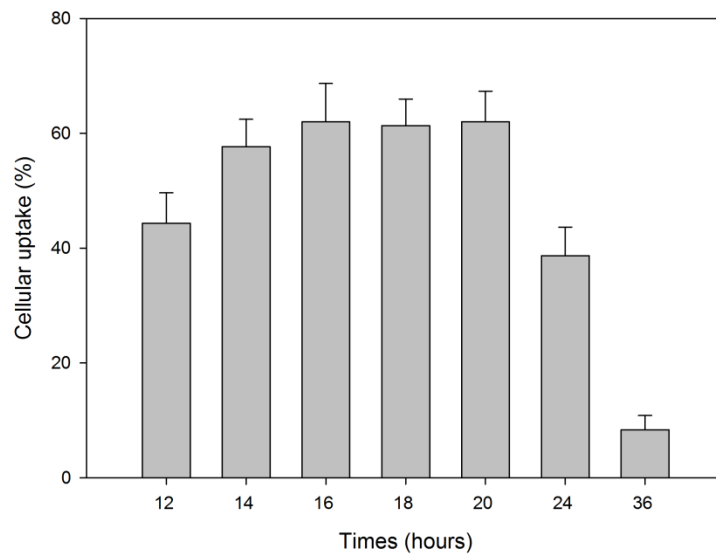


Figure S6: The effect of yeast growth time on cellular uptake of positively-charged nanosensors (15 mg/mL). Yeast cells were normally grown for different times (12-36 hours) before incubation with nanosensors and the number of fluorescent yeast cells, loaded with nanosensors, was counted in the red channel of the fluorescence microscope and compared to the control, counted in the brightfield mode.

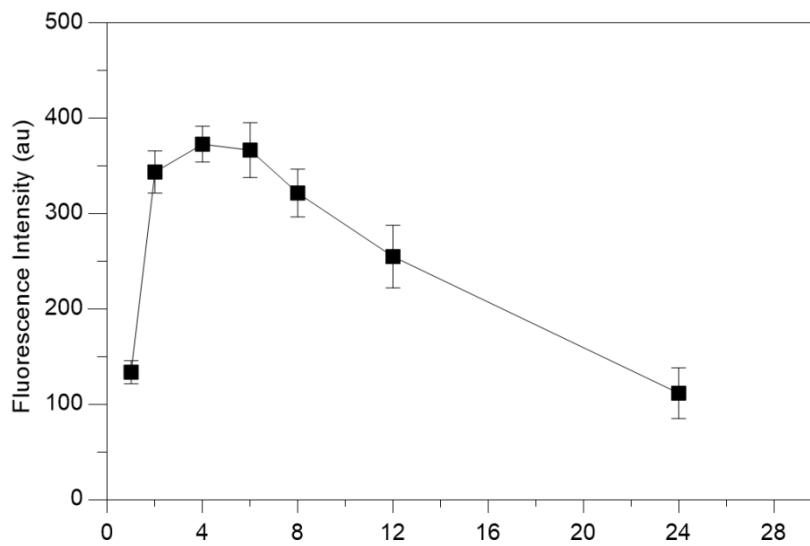


Figure S7: Effect of different incubation time between yeast and positively-charged nanosensors (15 mg/mL) on cellular uptake. Fluorescence intensity of TAMRA ($\lambda_{ex}=545$ nm, $\lambda_{em}=575$ nm) was used as an indicator for cellular uptake and 4 hours incubation was selected as the optimised incubation time. Error bars represent standard deviation, where n=3.

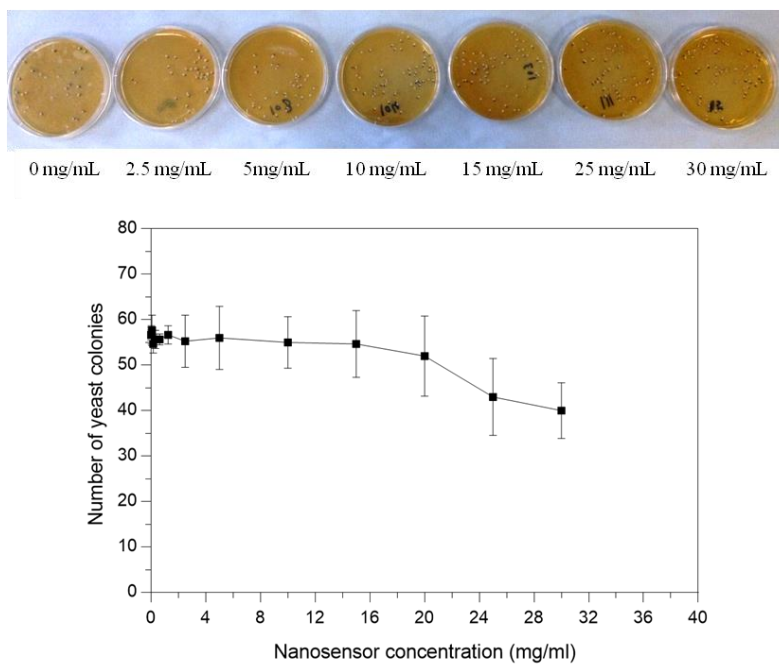
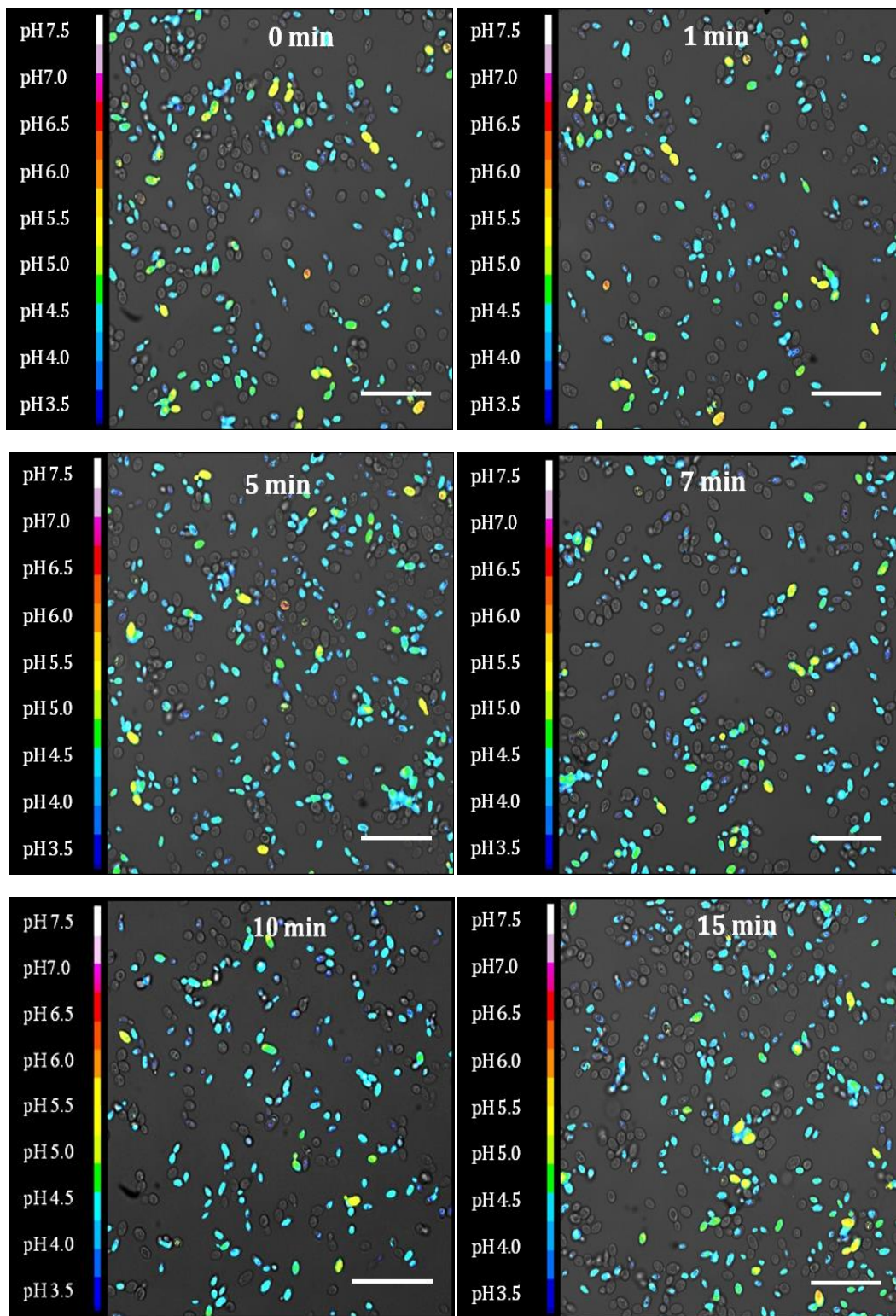


Figure S8: Toxicity study of yeast, incubated with different concentrations of positively-charged nanosensors, using the colony forming unit (CFU) test³. The image shows Petri dishes for yeast colonies after incubation with different nanosensor concentrations. The graph shows the number of yeast colonies using at increasing nanosensor concentration, when compared to the control, yeast without nanosensors. Error bars represent standard deviation, where n=3.



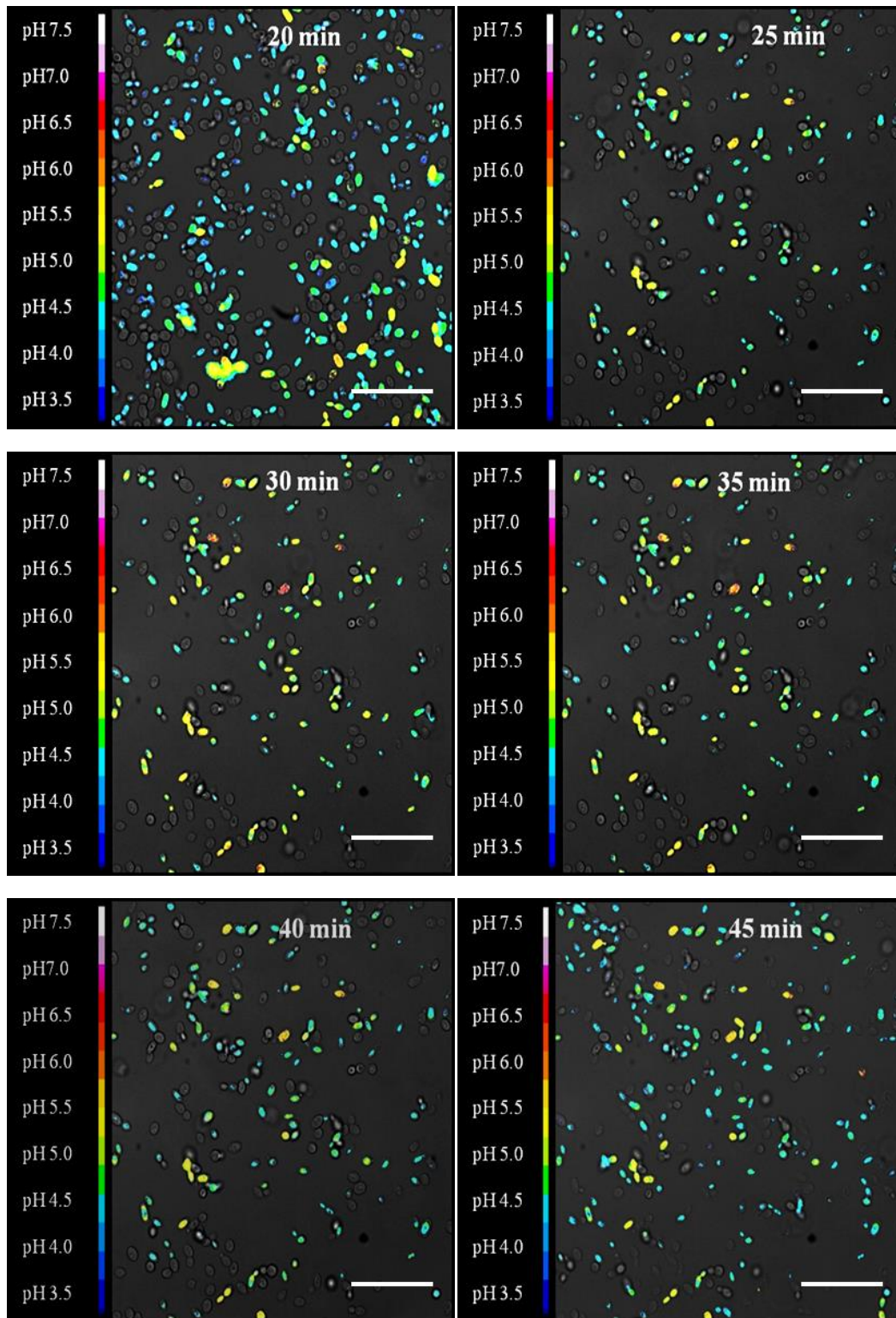


Figure S9: False colour heat map images of yeast loaded with positively-charged pH-sensitive nanosensors. Images were taken prior to glucose addition to glucose-starved yeast cells (0 min) and after consecutive time periods of glucose addition from 1 minute up to 45 minutes. The colour map images were established by ImageJ®. Scale bar = 50 μm.

References

- 1 Chauhan, V. M., Orsi, G., Brown, A., Pritchard, D. I. & Aylott, J. W. Mapping the pharyngeal and intestinal pH of *Caenorhabditis elegans* and real-time luminal pH oscillations using extended dynamic range pH-sensitive nanosensors. *ACS Nano***7**, 5577-5587, doi:10.1021/nn401856u (2013).
- 2 Jumpei Miyazaki *et al.* Adhesion and internalization of functionalized polystyrene latex nanoparticles toward the yeast *Saccharomyces cerevisiae*. *Advanced Powder Technology***25**, 1394–1397 (2014).
- 3 Nomura, T. *et al.* Exposure of the yeast *Saccharomyces cerevisiae* to functionalized polystyrene latex nanoparticles: influence of surface charge on toxicity. *Environ Sci Technol***47**, 3417-3423, doi:10.1021/es400053x (2013).